Key Points:
- The propagation of coastal trapped waves over a submarine canyon promotes upwelling over the shelf
- The upwelling is intensified over the downwave (upwave) side of the canyon during the low (high) sea level phase
- Accumulated upwelling results in a dense pool of upwelled water spread mainly in the downwave region

Circulation and Upwelling Induced by Coastal Trapped Waves Over a Submarine Canyon in an Idealized Eastern Boundary Margin

Gonzalo S. Saldías[1,2,3] , **Karina Ramos-Musalem**[2,4] , **and Susan E. Allen**[2]

[1]Departamento de Física, Facultad de Ciencias, Universidad del Bío-Bío, Concepción, Chile, [2]Department of Earth, Ocean and Atmospheric Sciences, University of British Columbia, Vancouver, Canada, [3]Centro FONDAP de Investigación en Dinámica de Ecosistemas Marinos de Altas Latitudes (IDEAL), Valdivia, Chile, [4]Centro de Ciencias de la Atmósfera, Universidad Nacional Autónoma de México, Ciudad de México, México

Abstract Wind-driven upwelling promotes the onshore transport of dense slope waters onto the continental shelf. New observational evidence suggests that the propagation of coastal trapped waves (CTWs) over a submarine canyon can also cause upwelling within the canyon, independent of the wind forcing. Here, we use idealized numerical experiments to assess the role of CTWs in promoting the onshore transport of deeper waters onto the continental shelf. The experiments are forced with a 7-days period CTW. Overall, there is accumulated upwelled water in time with increased onshore transport during the low sea level phase of the CTWs. Most of the onshore flow is spread over the upwave side of the canyon during the low sea level phase, but it is advected further downwave during the subsequent high sea level phase. As a result, a dense pool of upwelled water is spread over the shelf extending primarily in the downwave direction.

Plain Language Summary There are several ways in which deep water can reach the shallower coastal ecosystem near shore. Recent observations show evidence that coastal trapped waves, which are a special type of wave that travels close to the coast always keeping the land on its right (left) side in the northern (southern) hemisphere, can bring this deep water near shore when they pass over submarine canyons. Submarine canyons are v-shaped features that cut across the continental shelf. In this work we use computer simulations of a coastal trapped wave passing over a submarine canyon to further study how this interaction can bring deep water onto the shelf. We found that while the trough of the wave passes over the canyon, deep water flows up towards the shelf, and the opposite happens when the crest passes over the canyon; however, more water flows up onto the shelf than water leaves during the crest passing. There is a net input of deep water onto the shelf. As both coastal trapped waves and submarine canyons are ubiquitous in the global coastal ocean, this novel mechanism may have an important role in balancing the nutrients and oxygen that reach the shelf ecosystems all around the world

1. Introduction

Submarine canyons are major barriers to the along-isobath geostrophic flow over the continental shelf (Allen & Durrieu de Madron, 2009). Thus, cross-isobath flow occurs regularly within and over submarine canyons (e.g., Allen et al., 2001; Kämpf, 2006; Klinck, 1988), which results in the exchange of water and tracers between deep/slope waters and the continental shelf (Allen, 2004; Allen & Hickey, 2010; Ramos-Musalem & Allen, 2019; Skliris et al., 2001). Since submarine canyons present increased ageostrophic circulation, their effects on cross-shelf exchanges potentially impact regional scales (Brink, 2016; Connolly & Hickey, 2014). For instance, estimates of upwelling induced by submarine canyons to the southern Vancouver Island and Washington shelves are similar or even higher than the contribution from wind-driven coastal upwelling (Connolly & Hickey, 2014; Hickey & Banas, 2008). In general, numerous studies have analyzed the circulation associated with submarine canyons in eastern boundary margins (e.g., Hickey, 1997; Relvas et al., 2007; She & Klinck, 2000). Nonetheless, few studies have inspected the role of the interaction of a canyon with other shelf processes, such as the propagation of CTWs (Allen et al., 2001;Codiga et al., 1999; Sobarzo et al., 2016).

Eastern ocean boundary systems cover a small proportion of oceanic area, yet they support high biological production and fisheries (Carr & Kearns, 2003). This high productivity is principally linked to the fertilization effect of coastal upwelling (Brink, 1983; Huyer, 1983). The propagation of CTWs can also modulate the nearshore productivity (Echevin et al., 2014; Saraceno et al., 2005) due to the large vertical displacements of the pycnocline (and nutricline) in the coastal ocean (e.g., Clarke, 1977; Nash & Moum, 2005). Different aspects of CTWs have been studied along eastern ocean boundaries (e.g., Connolly et al., 2014; Illig & Bachèlery, 2019; Enfield & Allen, 1980; Shaffer et al., 1997), yet, there is limited information on their dynamical interaction with submarine canyons. Laboratory and numerical experiments have shown that changes in alongshore topography produce partial scattering of CTWs (e.g., Wilkin & Chapman, 1990; Zhang & Yankovsky, 2016) and a net onshore flow in a canyon forced with oscillatory alongshore currents (Boyer et al., 2004; Haidvogel, 2005). In general, the presence of a canyon would not affect, to a large extent, the alongshore propagation of the original wave (Codiga et al., 1999). Recent observations at the head of the Biobio River canyon show that significant upwelling cooling events (isotherms with vertical displacements >100 m) occur in response to the propagation of CTWs during weak local wind conditions (Sobarzo et al., 2016). This evidence suggests that CTWs could have a considerable impact on the circulation and upwelling within and around a submarine canyon.

This study aims to clarify the circulation and upwelling process associated with the propagation of CTWs over a submarine canyon in an idealized eastern boundary. We extend the time-mean results from previous studies that considered oscillatory barotropic flow resembling tidal currents (Haidvogel, 2005) by inspecting the period-averaged as well as low and high sea level cross-shelf exchange structure and transport. The primary focus is to describe the overall impact of low-frequency CTWs, uncoupled from the wind forcing, on promoting upwelling of slope/deep water over the continental shelf. Section 2 describes the numerical experiments using the Regional Ocean Modeling System (ROMS). Section 3 contains the main results and discussion in the context of previous studies and future approaches for observational studies, whereas the conclusions are highlighted in section 4.

2. Model Configuration and Experiments

The numerical experiments are run in ROMS, a model that solves the hydrostatic nonlinear primitive equations (Haidvogel et al., 2000). ROMS uses terrain-following s coordinates for the vertical discretization. The model is configured with a third-order upstream horizontal and a fourth-order centered vertical advection scheme for momentum and tracers. Note that high order advection is necessary to avoid spurious vertical velocities at the canyon rim due to stratified flow over steep topography using s coordinates (Allen et al., 2003). The horizontal pressure gradient is treated with a spline density Jacobian (Shchepetkin & McWilliams, 2003). Vertical mixing follows the Mellor-Yamada level 2.5 closure scheme (Mellor & Yamada, 1982); the background vertical viscosity and diffusivity are 1×10^{-5} m^2 s^{-1} and 5×10^{-6} m^2 s^{-1}, respectively. Bottom stress is calculated with a quadratic drag law using a bottom roughness of 2×10^{-2} m. Vertical resolution is supplied by 30 sigma levels with an increased resolution near the surface and bottom in order to resolve the surface and bottom boundary layers. The Coriolis parameter corresponds to 45°N ($f = 1.028 \times 10^{-4}$ s^{-1}).

The model domain is a rectangular basin resembling the coastal ocean of an eastern boundary in the northern hemisphere with 400 and 800 km in the cross-shore and alongshore direction, respectively (Figure 1). Grid spacing increases in the offshore direction from 0.2 km nearshore ($-50 < x < 0$ km) to ~12 km at the offshore boundary (Figure 1a, top panel), whereas a fixed 0.2 km of grid spacing is set in the alongshore direction over the shelf and slope $-50 < y < 50$ km, which increases up to 12 km farther away toward the northern and southern boundaries (Figure 1a, right panel). Different shelf-slope configurations were tested with all cases having a maximum depth of 500 m in the open ocean. We used a basic configuration following the bathymetry of Klinck (1996), which is defined by:

$$H(x, y) = H_m - \frac{H_s}{2}\left[1 - \tanh\frac{-x - x_o(y)}{a}\right] \tag{1}$$
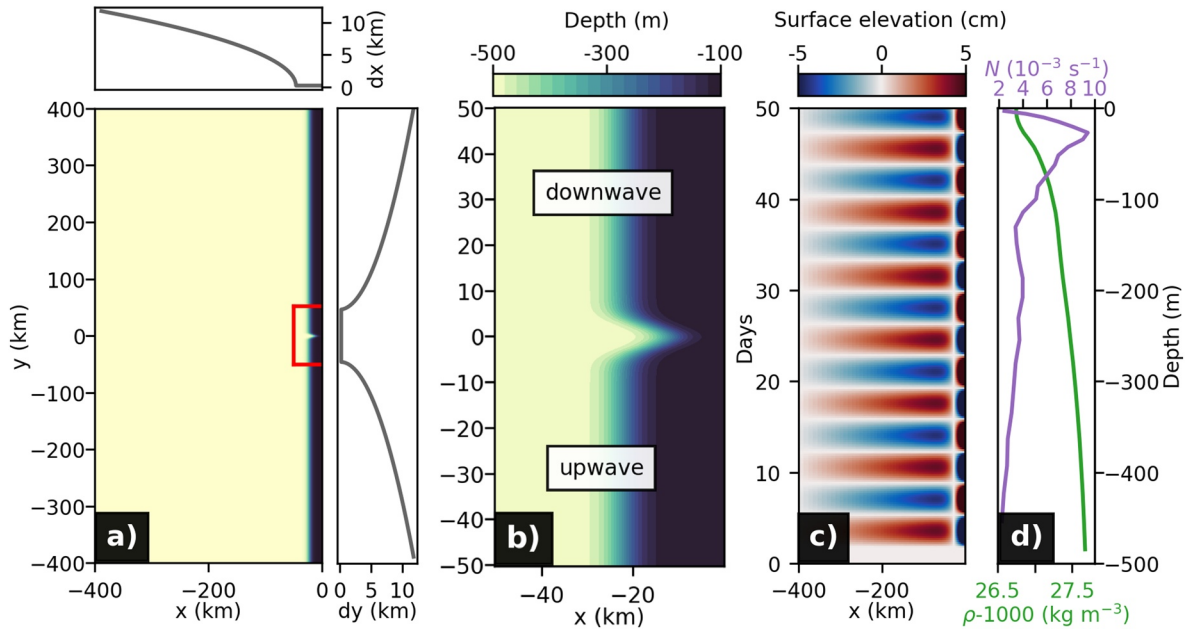
Figure 1. (a) Model domain bathymetry (colors, in m) of the base case (Deep and flat shelf) with the location of the submarine canyon enclosed in a red box, and shown in (b). The top and right panels in (a) show the variation of grid spacing in the x and y directions, respectively. The temporal evolution of the surface elevation (first mode of a CTW with a 7-day period) imposed at the southern boundary is shown in (c). The initial conditions of density and stratification (buoyancy frequency) are shown in (d). CTW, coastal trapped waves.

where H_m is the maximum depth of the domain (500 m), H_s is the depth change from the continental shelf to the open ocean (400 m), a is the transition scale defining the slope of the cross-shelf profile (5 km), and $x_o(y)$ is the location of the shelf break, defined as:

$$x_o(y) = x_n + x_b \left[1 - \exp \frac{-(y^2 - y_o^2)}{2b^2} \right] \qquad (2)$$

where x_n is the nominal distance of the head of the canyon from the coastal wall (12 km), x_b is the distance added to x_n to reach the shelf break (10 km), y_o is the location of the center of the canyon (at $y = 0$), and $b = 2.5$ km scales the width of the canyon (W). This configuration produces a canyon $\sim$10 km wide at its mouth and 20 km long from its mouth to the head (Figure 1b), analog to other shelf-break canyon studies (e.g., Kämpf, 2007, 2009; Klinck, 1996). The first baroclinic radius of deformation ($a_1 = NH/f$) on the shelf is between 5.5 and 9.3 km, which indicates that the canyon is dynamically narrow, following the criterion $W < 2a_1$ (Allen & Hickey, 2010). Two other bathymetry configurations with higher shelf slope are also studied (Figures 2b and 2c). Experiments with and without a submarine canyon are run to assess their differences.

The domain has three open boundaries (north, south, and offshore). A zero gradient condition is applied to the surface elevation on the western boundary, whereas the Orlanski radiation scheme (Orlanski, 1976) is applied for the rest of the variables. At the southern boundary, the local first mode CTW solutions are imposed for surface elevation and velocity fields. These CTW fields are obtained from running the code of Brink (2018), which uses the cross-shore bathymetry and stratification profile as input variables. The time variability of the wave fields is specified as a sine function with a wave period of 7 days (see Figure 1c). We choose to look for 7-days CTWs in analogy to the waves inducing enhanced upwelling on the Biobio Canyon (Sobarzo et al., 2016). These waves have wavelength $\sim$900 km ($\sim$90 times the width of the canyon). At the northern boundary, all variables are radiated using the Orlanski radiation conditions, which seems to be the best option for radiating long waves out of the downwave boundary (e.g., Dinniman & Klinck, 2002; Zhang & Yankovsky, 2016). Here we define downwave as the direction of propagation of long CTWs.
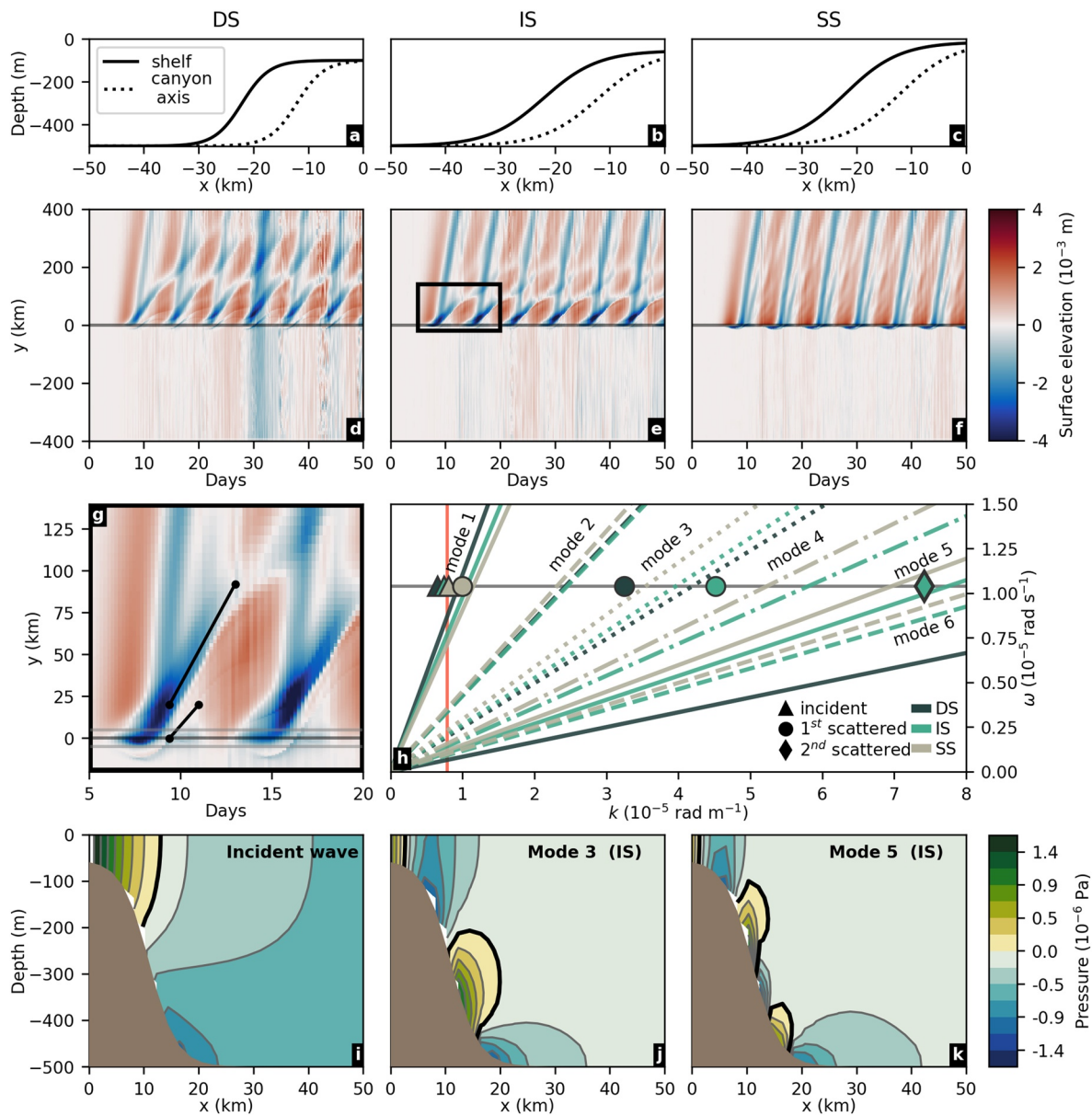
Figure 2. Difference between canyon runs and no-canyon runs (CR-NCR) for (d–f) alongshore sea level next to the coast for the three bathymetry configurations (a–c); solid and dashed black lines correspond to the along-canyon and ambient shelf profiles, respectively. The slope of the scattered signals for the IS case (black lines in g) is close to the speed of allowed wave modes 3 (j) and 5 (k). The cross-shore pressure field for the incident wave (mode 1), mode 3 and mode 5 calculated using the code by Brink (2018) are shown in (i), (j), and (k), respectively. The dispersion curves for allowed modes 1–6 for the three bathymetries as well as the scattered waves found are shown in (h).

3. Results and Discussion

The propagation of CTWs along the three contrasting bathymetry configurations (Figures 2a–2c) is affected by the presence of a submarine canyon, promoting the propagation of a trapped wave signal in the down-wave direction. Figures 2d–2f shows the difference in surface elevation from canyon and no-canyon runs (CR-NCR) next to the coast, where the original CTW (with faster propagation) is seen mainly with positive values (since the low sea level is lower in the NCR; Figures 2d–2f) and a secondary (and slower) CTW is generated from the submarine canyon and seen as the negative propagating field cutting across the positive anomalies (clearly seen for the Deep and Intermediate Shelf cases; Figures 2d and 2e). Although this new variability in sea level is detected downwave of the canyon through the difference (CR-NCR) in sea level, the

propagation of the main trapped wave is only weakly affected, which is in agreement with a previous study evaluating the impact of a canyon on wave propagation (Codiga et al., 1999). The analysis of the potential higher modes developed for all bathymetry configurations clarifies the process of scattering at the canyon generating slower trapped waves in the downwave direction (Figure 2h). A closer inspection of the speed of the scattered waves in the Intermediate Shelf case (Figures 2e and 2g) reveals the generation of mainly mode 3 and mode 5 CTWs at the canyon (Figures 2g and 2h). The vertical structure of these new waves is primarily bottom-trapped as seen in the subsurface pressure fields (Figures 2j and 2k). The increased bottom trapping at higher modes is consistent with a smaller offshore length scale subject to stronger bottom trapping for the same baroclinic radius of deformation (Wang & Mooers, 1976).

Cross-canyon sections of zonal velocities are presented in Figure 3 for all canyon experiments and during contrasting sea level heights on the canyon axis. A period-averaged (over three wave periods) cross-shore velocity field clarifies the residual onshore flow within and over the submarine canyon. A net onshore flow dominates the area over the canyon and is stronger in the Deep Shelf case (Figures 3b–3d). As already mentioned, canyon upwelling is dominant during the negative phase (low sea level) of the CTW, being intensified on the downwave side of the canyon (Figures 3h–3j). These results provide additional details to the upwelling structure associated with CTW-induced upwelling observed in moorings over the Biobio Canyon (Sobarzo et al., 2016), where similarly upwelling was only observed during negative phases of CTWs. Thus, in contrast with the classic schematic of canyon-driven upwelling on the upwave wall of a submarine canyon (Ramos-Musalem & Allen, 2019; Saldías & Allen, 2020), intensified CTW-driven upwelling occurs predominantly on the downwave wall during a negative sea level phase with onshore (Figures 3h–3j) and upward flow (Figure 3k–3m). Under the opposite phase with high sea level next to the coast, upwelling is still important but restricted to approximately the upwave half of the canyon (Figures 3e–3g). Thus, observational efforts should consider placing moorings on both sides of a canyon to accurately quantify the onshore upwelling flow, which is usually overlooked, during the high sea level phase of CTW propagation. In our experiments, the values of incoming velocity during the upwelling-favorable phase of the wave are between 0.05 and 0.1 m s^{-1}. Depending on the width W considered (at mid-length, at the shelf break, or mid-length at the rim depth isobath) and U for each shelf bathymetry, the Rossby number ($Rw = U/fW$) is between 0.05 and 0.2. These values are very close to the equivalent Rw in Kämpf (2009) (0.05–0.25) and lower but close to the equivalent values of Sobarzo et al. (2016) (0.13–0.31).

A more detailed inspection of the Intermediate Shelf results clarifies the distribution of upwelling waters over the shelf as a result of the passage of the 7-days period CTWs (Figure 4). The average density difference (CR-NCR) over the shelf shows an oscillating but progressively increasing density difference in time (Figure 4a). It is the result of the increased integrated onshore transport when a canyon is present (Figure 4b). The residual bottom density field, in the presence of a submarine canyon (more clearly seen through the difference CR-NCR), shows a density plume extending mostly in the downwave direction (Figure 4c). Nonetheless, its upwave impact is not negligible extending about 15 km south of the canyon (Figures 4c and 4i). In fact, a larger vertical extension with positive density differences (denser water in the presence of the canyon) occurs on the upwave side of the canyon during the low sea level phase (Figure 4j). During the following high sea level phase, the denser plume occupies about less than half of the water column in the downwave direction (Figure 4k), whereas less dense water is found above the canyon axis (Figures 4h and 4k; negative anomalies at $y = 0$ km). Thus, on average, the accumulated upwelling effect that CTWs have through a submarine canyon is primarily distributed over the downwave region (in the same direction of propagation of the CTW). Similar time-average bottom density anomalies were found by Haidvogel (2005) after forcing a canyon experiment with oscillatory barotropic currents resembling tidal flow. Nonetheless, its anomalous density field presented a relatively symmetric shape on either side of the canyon (see Haidvogel, 2005, Figures 3 and 4), which differs considerably from the density field in this study in response to CTWs.

The evolution of the upwelling process occurs as follows: During a low sea level phase the upwelling plume over the downwave side of the canyon is transported south (upwave; Figure 4d) in response to the southward alongshore flow associated with the low sea level next to the coast. The transition to a high sea level involves the advection of the previously upwelled water farther downwave, which results in an extended pool of high density water over the downwave region (Figure 4e). Comparing the CTW results to a wind-driven
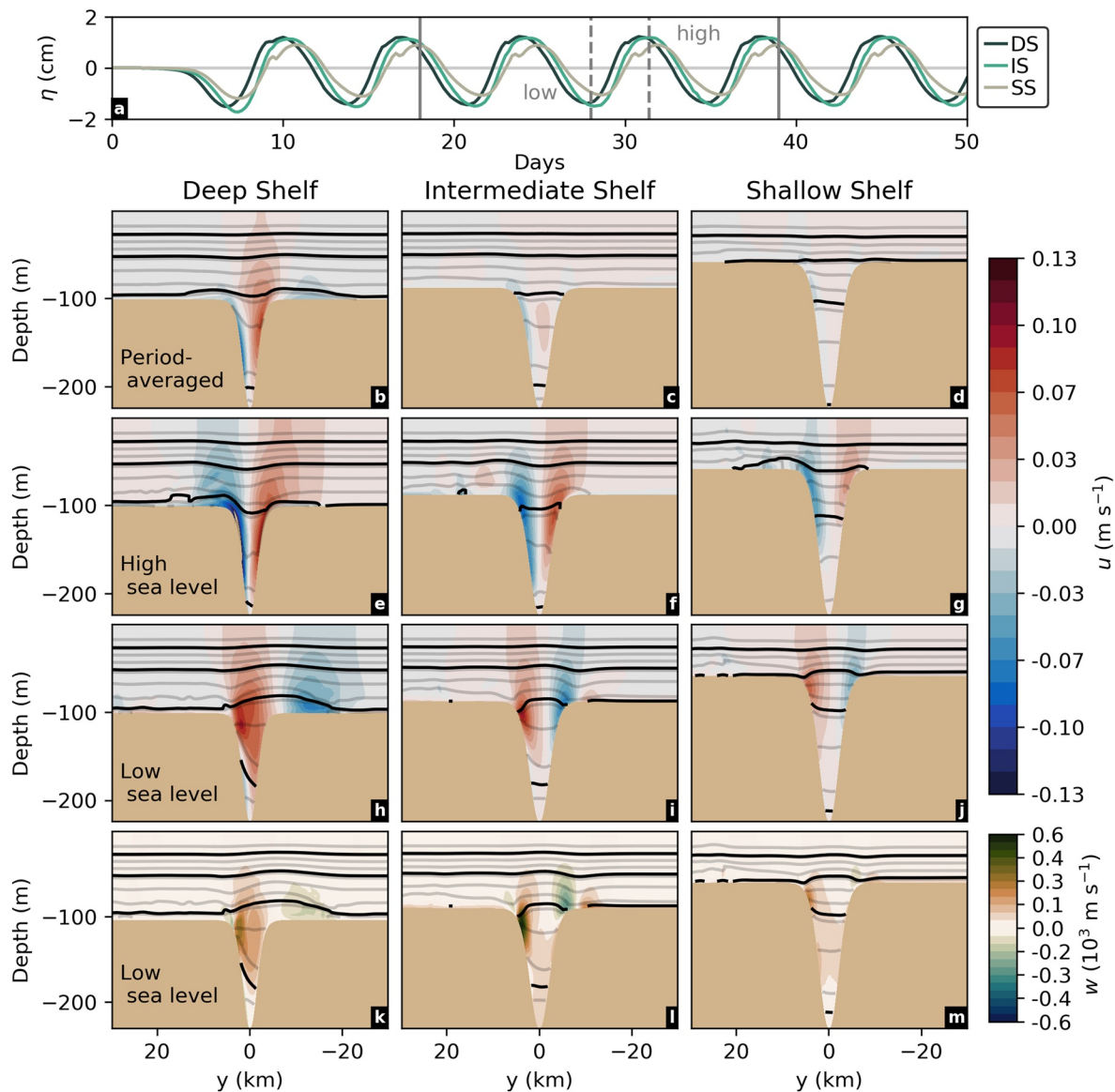
Figure 3. (a) Evolution of sea level next to the coast at $y = 0$ km (canyon axis) for the three bathymetry configurations (color coded) with a submarine canyon. The solid vertical gray lines denote the start and end of the computation of period-averaged cross-shore velocity fields (three wave periods), and the dashed vertical gray lines denote the selected events of low and high sea level, respectively. Cross-shore velocity fields are shown for (b)–(d) specified period-averaged, (e)–(g) high sea level, and (h)–(j) low sea level events through an alongshore plane along $x = -10$ km cutting across the submarine canyon ($-30 < y < 30$ km). Vertical velocity fields are shown for the same sections in (k–m). Black isopycnals correspond to σ levels 27.6, 27.8, 28.0, and 28.2 kg m^{-3}, and gray isopycnals are every 0.07 kg m^{-3}.

upwelling simulation with the same bathymetries (Saldías & Allen, 2020), we note that the adjustment time of flow over the canyon to wind-driven forcing is on the order of days. The CTW's, with a period of 7 days, are accelerating/decelerating on a time scale similar to the adjustment time. The incoming flow is not steady over the canyon when forced by CTWs. Consequently, the circulation is highly time-dependent switching between the low and high sea level phase of the CTWs. The circulation structure in the canyon during the low sea level phase is very similar to that of the wind-driven case during the initial forcing stage (see S1, supporting information) or time-dependent upwelling phase (Allen & Hickey, 2010), but then there is no time for the canyon to develop into the advective phase because the flow is reversed (see Table 1 for additional comparisons).
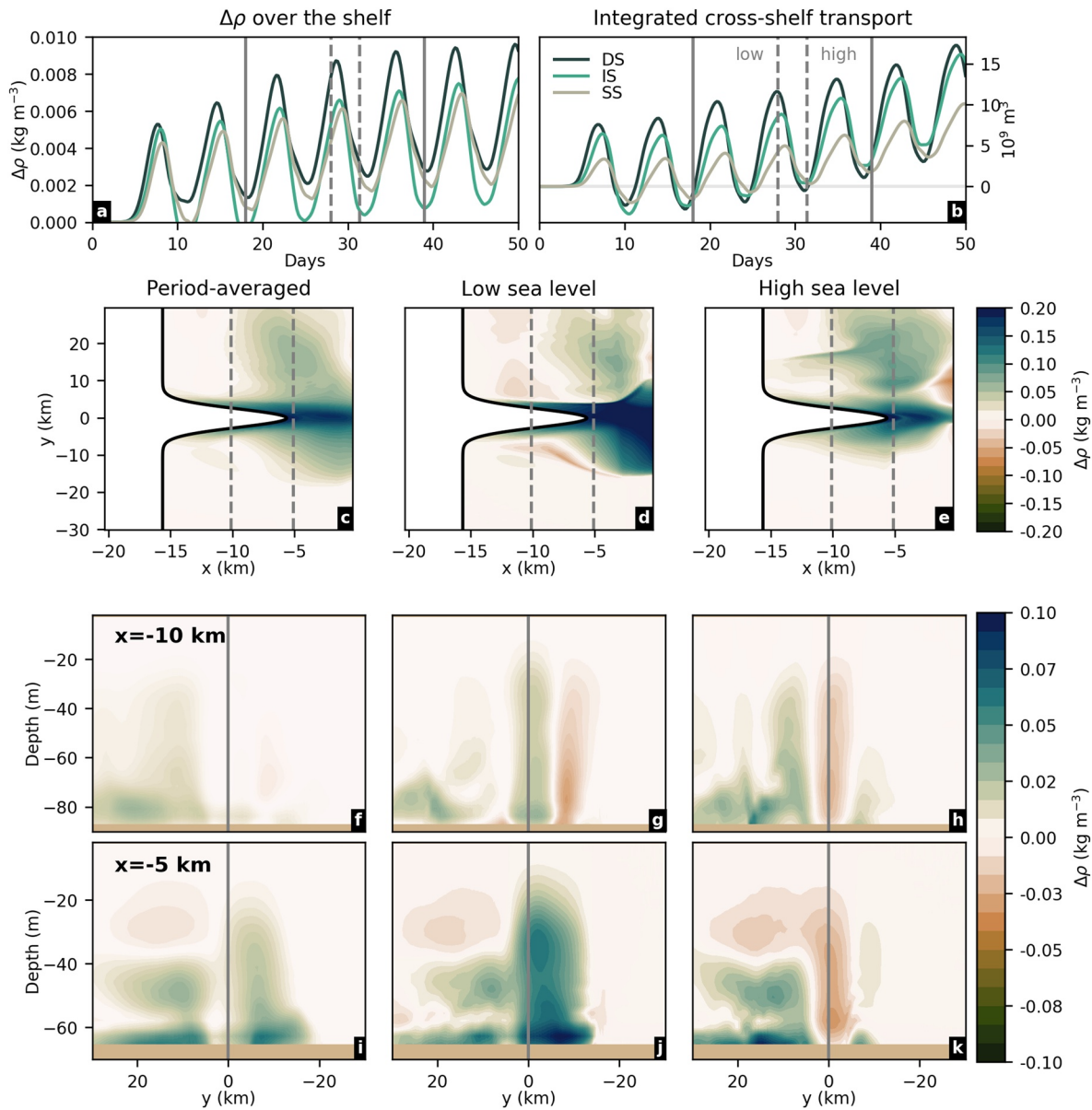
Figure 4. Evolution of (a) difference (CR-NCR) in density over the shelf (volume limited offshore by the 150 m isobath and $-30 < y < 30$ km), and (b) integrated cross-shore transport through the alongshore plane delimited by the 150 m isobath from $-30 < y < 30$ km (canyon runs). Solid gray lines indicate the averaging period (c, f, i) and dashed lines show the times of low and high sea level (all other panels). The difference (CR-NCR) in (c)–(e) bottom density, (f)–(h) density at 10 km from the coast, and (i)–(k) density at 5 km from the coast are presented for the selected period-averaged, low sea level, and high sea level events of Intermediate Shelf experiments, respectively.

CTW-driven upwelling events have potentially important biological consequences near the bottom since mass die-offs of benthic organisms have been linked to the upwelling of hypoxic slope waters over the shelf of an eastern boundary (Hernández-Miranda et al., 2012). As seen in the study of Sobarzo et al. (2016), a train of several CTWs were recorded to generate upwelling in the canyon, and thus, a cumulative on-shore transport of dense (and hypoxic) waters can be spread over the shelf even in the absence of any up-welling-favorable wind forcing. Considering that other tracers (such as nutrients) are also carried onshore during the upwelling process (Ramos-Musalem & Allen, 2020), the propagation of CTWs near submarine canyons could have important biogeochemical impacts on the continental shelf. Future observational stud-ies should take into consideration the spatial distribution of the onshore flow according with the phase of a trapped wave—placing a mooring over both upwave and downwave sides of a canyon would be appropriate

Table 1
Summary of Flow Features Induced by CTW-Driven Upwelling/Downwelling and Wind-Driven Upwelling in a Submarine Canyon

Feature	Wind-driven upwelling	CTW-driven upwelling	CTW-driven downwelling
Surface elevation	low	low	high
Incoming flow	upwave/southward	upwave/southward	downwave/northward
CS circulation	cyclonic (advection-driven)	anticyclonic (time-dependent)	cyclonic and more symmetric
Vertical velocity	mostly positive (upwave side)	mostly positive (downwave side)	mostly negative (downwave side)
Upwelled water distribution	only upwave (downstream)	mostly upwave	mostly downwave

CS, Cross-shelf; CTW, coastal trapped waves.

to measure the intensified upwelling flow driven by CTWs. Finally, the inclusion of upwelling-favorable wind forcing in our experiments would add valuable new insights regarding their potential accumulated effect (CTW plus wind-driven upwelling) transporting anomalous dense water over the shelf.

4. Summary and Conclusions

Although they lead to significant upwelling of slope waters onto the continental shelf, the impact of CTWs driving canyon-upwelling has been largely overlooked. Motivated by recent observational findings of strong upwelling (with isotherms rising more than 100 m) over the head of the Biobio Canyon off central Chile, we performed a series of numerical experiments to evaluate the upwelling response that propagating CTWs generate over an idealized canyon placed in an eastern boundary shelf.

Residual (CR-NCR) sea level elevation fields reveal that the canyon promotes the downwave propagation of slower CTW modes. The original forced CTW is, in general, barely affected by the presence of a submarine canyon. Nonetheless, upwelling of denser waters over the shelf is channeled along the downwave side of the canyon during the low sea level phase of the wave. A net offshore transport occurs during the opposite (high) sea level phase. However, local onshore flow is still important over the upwave canyon wall. The accumulated dense pool of upwelled water is primarily spread in the downwave direction as a result of the dominant downwave flow during the positive CTW phase. This upwelled water distribution differs from the more classical wind-driven upwelling in a canyon where the dense pool is spread on the downstream (upwave) shelf.

Data Availability Statement

Data files are archived in the Zenodo repository (https://doi.org/10.5281/zenodo.4750205).

References

Allen, S. E. (2004). Restrictions on deep flow across the shelf-break and the role of submarine canyons in facilitating such flow. *Surveys in Geophysics*, *25*(3–4), 221–247. https://doi.org/10.1007/s10712-004-1275-0

Allen, S. E., Dinniman, M., Klinck, J., Gorby, D., Hewett, A., & Hickey, B. (2003). On vertical advection truncation errors in terrain-following numerical models: Comparison to a laboratory model for upwelling over submarine canyons. *Journal Geophysical Research*, *108*(C1), 3–1. https://doi.org/10.1029/2001JC000978

Allen, S. E., & Durrieu de Madron, X. (2009). A review of the role of submarine canyons in deep-ocean exchange with the shelf. *Ocean Science*, *5*(4), 607–620. https://doi.org/10.5194/os-5-607-2009

Allen, S. E., & Hickey, B. (2010). Dynamics of advection-driven upwelling over a shelf break submarine canyon. *Journal of Geophysical Research*, *115*(C8). https://doi.org/10.1029/2009JC005731

Allen, S. E., Vindeirinho, C., Thomson, R., Foreman, M. G., & Mackas, D. (2001). Physical and biological processes over a submarine canyon during an upwelling event. *Canadian Journal of Fisheries and Aquatic Sciences*, *58*(4), 671–684. https://doi.org/10.1139/f01-008

Boyer, D. L., Haidvogel, D. B., & Pérenne, N. (2004). Laboratory–numerical model comparisons of canyon flows: A parameter study. *Journal of Physical Oceanography*, *34*(7), 1588–1609. https://doi.org/10.1175/1520-0485(2004)034<1588:lmcocf>2.0.co;2

Brink, K. H. (1983). The near-surface dynamics of coastal upwelling. *Progress in Oceanography*, *12*(3), 223–257. https://doi.org/10.1016/0079-6611(83)90009-5

Brink, K. H. (2016). Cross-shelf exchange. *Annual Review of Marine Science*, *8*, 59–78. https://doi.org/10.1146/annurev-marine-010814-015717

Brink, K. H. (2018). *Stable coastal-trapped waves with stratification, topography and mean flow in matlab (Tech. Rep.)*, Woods Hole Oceanographic Institution. https://hdl.handle.net/1912/10527

Carr, M., & Kearns, E. J. (2003). Production regimes in four eastern boundary current systems. *Deep-Sea Research II*, *50*(22), 3199–3221. https://doi.org/10.1016/j.dsr2.2003.07.015

Clarke, A. (1977). Wind-forced linear and nonlinear Kelvin waves along an irregular coastline. *Journal of Fluid Mechanics*, *83*(2), 337–348. https://doi.org/10.1017/s0022112077001220

Codiga, D., Renouard, D. P., & Fincham, A. M. (1999). Experiments on waves trapped over the continental slope and shelf in a continuously stratified rotating ocean, and their incidence on a canyon. *Journal of Marine Research*, *57*(4), 585–612. https://doi.org/10.1357/002224099321549602

Connolly, T., & Hickey, B. M. (2014). Regional impact of submarine canyons during seasonal upwelling. *Journal Geophysical Research: Oceans*, *119*(2), 953–975. https://doi.org/10.1002/2013JC009452

Connolly, T., Hickey, B. M., Shulman, I., & Thomson, R. E. (2014). Coastal trapped waves, alongshore pressure gradients, and the California undercurrent. *Journal of Physical Oceanography*, *44*(1), 319–342. https://doi.org/10.1175/jpo-d-13-095.1

Dinniman, M. S., & Klinck, J. M. (2002). The influence of open versus periodic alongshore boundaries on circulation near submarine canyons. *Journal of Atmospheric and Oceanic Technology*, *19*(10), 1722–1737. https://doi.org/10.1175/1520-0426(2002)019<1722:tioovp>2.0.co;2

Echevin, V., Albert, A., Lévy, M., Graco, M., Aumont, O., Piétri, A., & Garric, G. (2014). Intraseasonal variability of nearshore productivity in the northern Humboldt Current System: The role of coastal trapped waves. *Continental Shelf Research*, *73*, 14–30. https://doi.org/10.1016/j.csr.2013.11.015

Enfield, D., & Allen, J. S. (1980). On the structure and dynamics of monthly mean sea level anomalies along the Pacific coast of North and South America. *Journal of Physical Oceanography*, *10*(4), 557–578. https://doi.org/10.1175/1520-0485(1980)010<0557:otsado>2.0.co;2

Haidvogel, D. B. (2005). Cross-shelf exchange driven by oscillatory barotropic currents at an idealized coastal canyon. *Journal of Physical Oceanography*, *35*(6), 1054–1067. https://doi.org/10.1175/jpo2735.1

Haidvogel, D. B., Arango, H. G., Hedstrom, K., Beckmann, A., Malanotte-Rizzoli, P., & Shchepetkin, A. F. (2000). Model evaluation experiments in the north Atlantic basin: Simulations in nonlinear terrain-following coordinates. *Dynamics of Atmospheres and Oceans*, *32*(3–4), 239–281. https://doi.org/10.1016/s0377-0265(00)00049-x

Hernández-Miranda, E., Veas, R., Labra, F. A., Salamanca, M., & Quiñones, R. A. (2012). Response of the epibenthic macrofaunal community to a strong upwelling-driven hypoxic event in a shallow bay of the southern Humboldt Current System. *Marine Environmental Research*, *79*, 16–28. https://doi.org/10.1016/j.marenvres.2012.04.004

Hickey, B. (1997). The response of a steep-sided, narrow canyon to time-variable wind forcing. *Journal of Physical Oceanography*, *27*(5), 697–726. https://doi.org/10.1175/1520-0485(1997)027<0697:troass>2.0.co;2

Hickey, B., & Banas, N. (2008). Why is the northern end of the California Current System so productive? *Oceanography*, *21*(4), 90–107. https://doi.org/10.5670/oceanog.2008.07

Huyer, A. (1983). Coastal upwelling in the California Current system. *Progress in Oceanography*, *12*(3), 259–284. https://doi.org/10.1016/0079-6611(83)90010-1

Illig, S., & Bachèlery, M.-L. (2019). Propagation of subseasonal equatorially-forced coastal trapped waves down to the Benguela upwelling system. *Scientific Reports*, *9*(1), 5306. https://doi.org/10.1038/s41598-019-41847-1

Kämpf, J. (2006). Transient wind-driven upwelling in a submarine canyon: A process-oriented modeling study. *Journal Geophysical Research: Oceans*, *111*(C11). https://doi.org/10.1029/2006JC003497

Kämpf, J. (2007). On the magnitude of upwelling fluxes in shelf-break canyons. *Continental Shelf Research*, *27*(17), 2211–2223. https://doi.org/10.1016/j.csr.2007.05.010

Kämpf, J. (2009). On the interaction of time-variable flows with a shelfbreak canyon. *Journal of Physical Oceanography*, *39*(1), 248–260. https://doi.org/10.1175/2008jpo3753.1

Klinck, J. (1988). The influence of a narrow transverse canyon on initially geostrophic flow. *Journal Geophysical Research: Oceans*, *93*(C1), 509–515. https://doi.org/10.1029/JC093iC01p00509

Klinck, J. (1996). Circulation near submarine canyons: A modeling study. *Journal Geophysical Research*, *101*(C1), 1211–1223. https://doi.org/10.1029/95JC02901

Mellor, G. L., & Yamada, T. (1982). Development of a turbulence closure model for geophysical fluid problems. *Reviews of Geophysics*, *20*(4), 851–875. https://doi.org/10.1029/RG020i004p00851

Nash, J. D., & Moum, J. N. (2005). River plumes as a source of large-amplitude internal waves in the coastal ocean. *Nature*, *437*(7057), 400–403. https://doi.org/10.1038/nature03936

Orlanski, I. (1976). A simple boundary condition for unbounded hyperbolic flows. *Journal of Computer Science*, *21*, 251–269. https://doi.org/10.1016/0021-9991(76)90023-1

Ramos-Musalem, K., & Allen, S. E. (2019). The impact of locally-enhanced vertical diffusivity on the cross-shelf transport of tracers induced by a submarine canyon. *Journal of Physical Oceanography*, *49*, 561–584. https://doi.org/10.1175/jpo-d-18-0174.1

Ramos-Musalem, K., & Allen, S. E. (2020). The impact of initial tracer profile on the exchange and on-shelf distribution of tracers induced by a submarine canyon. *Journal Geophysical Research: Oceans*, *125*.

Relvas, P., Barton, E. D., Dubert, J., Oliveira, P. B., Peliz, A., Da Silva, J., & Santos, A. M. P. (2007). Physical oceanography of the western Iberia ecosystem: Latest views and challenges. *Progress in Oceanography*, *74*(2), 149–173. https://doi.org/10.1016/j.pocean.2007.04.021

Saldías, G. S., & Allen, S. E. (2020). The influence of a submarine canyon on the circulation and cross-shore exchanges around an upwelling front. *Journal of Physical Oceanography*, *50*(6), 1677–1698. https://doi.org/10.1175/jpo-d-19-0130.1

Saraceno, M., Provost, C., & Piola, A. R. (2005). On the relationship between satellite-retrieved surface temperature fronts and chlorophyll a in the western South Atlantic. *Journal Geophysical Research*, *110*(C11). https://doi.org/10.1029/2004JC002736

Shaffer, G., Pizarro, O., Djurfeldt, L., Salinas, S., & Rutllant, J. (1997). Circulation and low-frequency variability near the Chilean coast: Remotely forced fluctuations during the 1991–92 El Niño. *Journal of Physical Oceanography*, *27*(2), 217–235. https://doi.org/10.1175/1520-0485(1997)027<0217:calfvn>2.0.co;2

Shchepetkin, A. F., & McWilliams, J. C. (2003). A method for computing horizontal pressure-gradient force in an oceanic model with a nonaligned vertical coordinate. *Journal Geophysical Research*, *108*(C3). https://doi.org/10.1029/2001JC001047

She, J., & Klinck, J. M. (2000). Flow near submarine canyons driven by constant winds. *Journal of Geophysical Research*, *105*(C12), 28671–28694. https://doi.org/10.1029/2000JC900126

Skliris, N., Goffart, A., Hecq, J., & Djenidi, S. (2001). Shelf-slope exchanges associated with a steep submarine canyon off Calvi (Corsica, NW Mediterranean Sea): A modeling approach. *Journal Geophysical Research*, *106*(C9), 19883–19901. https://doi.org/10.1029/2000JC000534

Sobarzo, M., Saldías, G. S., Tapia, F. J., Bravo, L., Moffat, C., & Largier, J. L. (2016). On subsurface cooling associated with the Biobio River canyon (Chile). *Journal Geophysical Research: Oceans*, *121*, 4568–4584. https://doi.org/10.1002/2016JC011796

Wang, D.-P., & Mooers, C. N. (1976). Coastal-trapped waves in a continuously stratified ocean. *Journal of Physical Oceanography*, *6*(6), 853–863. https://doi.org/10.1175/1520-0485(1976)006<0853:ctwiac>2.0.co;2

Wilkin, J., & Chapman, D. C. (1990). Scattering of coastal-trapped waves by irregularities in coastline and topography. *Journal of Physical Oceanography*, *20*(3), 396–421. https://doi.org/10.1175/1520-0485(1990)020<0396:soctwb>2.0.co;2

Zhang, T., & Yankovsky, A. E. (2016). On the nature of cross-isobath energy fluxes in topographically modified barotropic semidiurnal Kelvin waves. *Journal Geophysical Research: Oceans*, *121*(5), 3058–3074. https://doi.org/10.1002/2015JC011617